Hanle Effect in the He-Ne Laser*

W. CULSHAW AND J. KANNELAUD
Research Laboratories, Lockheed Missiles and Space Company, Palo Alto, California
(Received 13 May 1964)

The effect of small magnetic fields on the degenerate levels of the 1.153-μ He-Ne laser transition is considered in the region where the transitions overlap and coherence is imparted by the excitation and induced-emission processes. Perturbation equations for the phenomena are solved by a small-signal approximation, and the probability amplitudes summed coherently to give the resultant intensity and polarization changes. For a symmetrical disposition of the laser frequency with respect to the Zeeman transitions, the polarization remains linear until the states separate beyond the natural linewidth, but rotates with increasing magnetic field. Rotations around 45° are indicated for axial and transverse magnetic fields less than one gauss. With the laser frequency asymmetric with respect to the transitions, elliptical polarization occurs. Investigations on a short planar laser show that such a rotation does take place when small axial magnetic fields are applied and that the polarization remains linear. Some variation with the rf level of excitation is encountered, and there are similar effects at a higher value of dc magnetic field. Studies with sawtooth and ac magnetic fields show the modulation and harmonics which result when the periodic rotation is passed through an analyzer. The separation beyond the natural linewidth is indicated by the appearance of circularly polarized beats at the extremes of the ac fields. The rotation consistently occurs with the laser tuned near the line center and operated well above threshold. When the laser frequency is removed from the center of the Doppler linewidth, the rotation is small or absent, and elliptical polarization has been observed.

1. INTRODUCTION

IN a previous paper[1] we have discussed Zeeman and coherence effects in gas lasers and, in particular, the Hanle effect,[2] which is concerned with the depolarization of resonance radiation in weak magnetic fields. Weisskopf,[3] and later Breit,[4] derived general expressions for the polarization of the fluorescent radiation in an arbitrary magnetic field, from which such depolarization effects can be deduced. These formulations deal with the coherent excitation of the scattering atom, and the polarization of the fluorescent radiation from the overlapping excited states. For the resonance line of mercury, with no hyperfine structure, the usual longitudinal Hanle effect can be interpreted as a coherent excitation of the σ_- and σ_+ transitions, and a subsequent coherent decay with a definite phase relationship between the resulting circularly polarized transitions to the ground state. This gives the observed linear polarization along the direction of the incident electric vector in zero magnetic field, and depolarization effects and a rotation of the plane of polarization as the magnetic field increases. We assume that highly monochromatic radiation is involved, as would be the case in considerations of such effects in the gas laser. For fluorescent radiation, however, the probability coefficient for the emission of a particular photon type must be integrated over the frequency width of the spontaneous emission, as was done by Breit,[4] in order to give the total radiation with a specific polarization. Thus, while some degree of similarity between the Hanle effect in the gas laser and that observed in resonance radiation will exist, we cannot expect that the results will agree precisely, even under similar conditions, with those given by the classical formulas for the depolarization of resonance radiation. Differences arise due to the highly monochromatic nature of the laser radiation, and to the induced emission processes which are effective.

The effects of small magnetic fields on the gas laser are given further consideration, both theoretically and experimentally, in this report, which will extend and augment a brief account of the work which has already appeared.[5] In such investigations the specific polarizations of the various transitions must be compatible with the photon types which the laser cavity can accept, in order that energy interchange can occur and oscillations build up. A planar or internal optics laser with no polarization constraint is thus suitable for such investigations, since oscillations will occur in any polarization depending on that of the atomic transitions involved. A resonator with an internal polarization constraint is less suitable for this work, since laser oscillation can only occur with a linear polarization whose direction is governed by the orientation of, say, Brewster angle windows.

A small-signal approximation is used to solve the equations for the probability amplitudes of the various Zeeman transitions in the laser. These are summed in a coherent way to give the resultant probability amplitude and polarization due to the overlapping transitions. Transition probabilities are then deduced, and the rotation of the plane of polarization of the laser radiation with magnetic field is determined. The results are compared with the analogous results on the depolarization of resonance radiation, and show that the polarization remains linear for Zeeman separations within the natural

* Research on report supported by the Independent Research Program of Lockheed Missiles and Space Company.
[1] W. Culshaw and J. Kannelaud, Phys. Rev. **133**, A691 (1964).
[2] A. C. G. Mitchell and M. W. Zemansky, *Resonance Radiation and Excited Atoms* (Cambridge University Press, New York, 1934), pp. 258–317.
[3] V. F. Weisskopf, Ann. Physik **9**, 23 (1931).
[4] G. Breit, Rev. Mod. Phys. **5**, 91 (1933).
[5] W. Culshaw and J. Kannelaud, Bull. Am. Phys. Soc. **9**, 65 (1964).

linewidth of the transitions, provided that the laser frequency is symmetrically disposed with respect to the $\Delta M=\pm 1$ transitions of a single atom. The polarization, however, rotates with increasing magnetic field, and the results predict a large effect with rotations up to 45° for magnetic fields less than 1 G. For other asymmetrical positions of the cavity resonance with respect to the transitions, elliptical polarization occurs. Some measurements on the phenomena have been made with a short planar laser operating at 1.153 μ in essentially a single axial mode, and these are in substantial agreement with the theory. Some additional verification of the theory is also provided by the independent work of Dumont and Durant,[6] who have used a pulsed He-Ne laser operating at 1.153 μ. In this work, small transverse magnetic fields are applied along the polarization in zero magnetic field (π mode). On increasing the magnetic field from zero and pulsing, a gradual decrease in the number of π mode oscillations and an increase in the number of σ oscillations from the initially equal numbers is observed corresponding to a rotation of the plane of polarization.

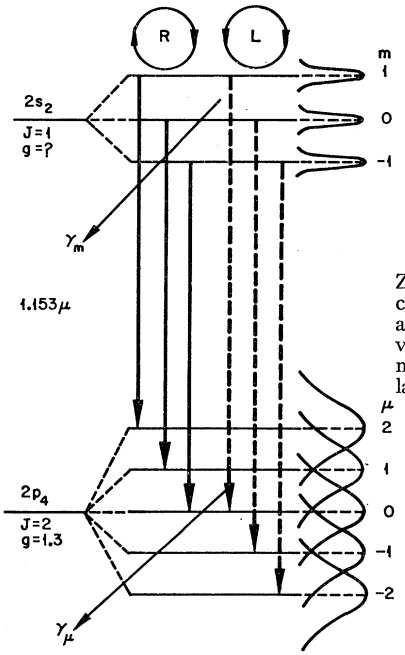

FIG. 1. Overlapping Zeeman levels, decay constants, transitions, and polarizations involved for an axial magnetic field on the laser.

2. THEORY

a. Axial Magnetic Field

The Zeeman splitting of the $2s_2 \rightarrow 2p_4$ laser transition at 1.153 μ is shown in Fig. 1. Allowed electric dipole transitions $\Delta M=0$, or ± 1 thus give nine transitions for a transverse magnetic field on the laser and six transitions for an axial magnetic field. The g values of the upper and lower levels will both be assumed equal to 1.3.[1] Such a restriction can be removed, but the computations become complicated. With a small axial magnetic field applied to the laser so that all such transitions overlap, we may sum the right- and left-handed circularly polarized transitions shown in a coherent way to obtain the resultant polarization of the composite transition. The direction of the magnetic field in Fig. 1 is towards the reader. A single atom is considered to be excited as a coherent mixture of the eigenstates $|m\rangle$ by the discharge at $t=0$. Under the assumption of equal g values, all transitions $\Delta M=\pm 1$ give angular frequencies which differ by $\pm geH/2mc$ from that given by $\omega\hbar_s=E_1-E_2$, where E_1 and E_2 are the energies of the upper state $|j=1, m=0\rangle$ and the lower state $|j=2, m=0\rangle$, respectively. The angular frequency of the laser radiation ω will be approximately equal to ω_s, and the symmetrical case occurs when $\omega=\omega_s$. Linear polarization results when $\omega=\omega_s$ and elliptical polarization when $\omega\neq\omega_s$. Since the levels overlap, the laser radiation can induce the transitions $\Delta M\pm 1$ in a coherent way, with some specific polarization determined by the resultant probability amplitude for all transitions. The largest measure of coherence will obviously be obtained when the upper levels overlap, and since we must have $geH/2mc<\gamma_m$, where $\gamma_m\approx 10^7$ sec^{-1}, it is apparent that large effects may be expected for small magnetic fields ≈ 1 G. As shown in Fig. 1 the levels $|m\rangle$ and $|\mu\rangle$ have decay constants γ_m and γ_μ to lower lying levels, which are introduced into the perturbation equations in a phenomenological way.[7,8] Coherence effects will occur for magnetic fields such that $geH/2mc<\gamma_m+\gamma_\mu$, but for higher values it will disappear, and the transitions $\Delta M=\pm 1$ will then occur independently with the normal circular polarizations.

The state vector of the atom may be written

$$|\ \rangle=\sum_m a_m e^{-iE_m t/\hbar}|m\rangle+\sum_\mu b_\mu e^{-iE_\mu t/\hbar}|\mu\rangle \qquad (1)$$

and Schrödinger's equation as

$$i\hbar d|\ \rangle/dt=(\mathcal{H}_0+\mathcal{H}_e)|\ \rangle, \qquad (2)$$

where $\mathcal{H}_e$ is the electric dipole perturbation $e\mathbf{E}(t)\cdot\mathbf{r}$. The equations for the probability amplitudes of the states are thus

$$\begin{aligned} \dot{a}_m&=(i\hbar)^{-1}\textstyle\sum_\mu H_{m\mu}e^{i\omega_{m\mu}t}b_\mu-a_m\gamma_m/2, \\ \dot{b}_\mu&=(i\hbar)^{-1}\textstyle\sum_m H_{\mu m}e^{i\omega_{\mu m}t}a_m-b_\mu\gamma_\mu/2. \end{aligned} \qquad (3)$$

Here,

$$\omega_{m\mu}=(E_m-E_\mu)/\hbar, \quad \text{and} \quad H_{m\mu}=\langle m|\mathbf{E}(t)\cdot\mathbf{r}|\mu\rangle, \qquad (4)$$

where $\mathbf{E}(t)$ is the electric field due to the laser radiation within the cavity, and the rotating wave approximation is used. The time-independent part of the matrix element in Eq. (4) will also be denoted by $H_{m\mu}$ in what follows. Consider first a two-level system which can be

[6] M. Dumont and G. Durand, Phys. Letters **8**, 100 (1964).

[7] V. F. Weisskopf and E. P. Wigner, Z. Physik **63**, 54 (1930).

[8] W. E. Lamb, Jr., and T. M. Sanders, Jr., Phys. Rev. **119**, 1901 (1960).

solved exactly for any magnitude of the perturbation. First, we apply a small signal theory and deduce $b_\mu(t)$ under the initial conditions $b_\mu(0)=0$, and $a_m(0)=1$. Under this assumption the probability amplitude a_m is given by

$$a_m(t)=a_m(0)e^{-\gamma_m t/2}, \tag{5}$$

the term involving $H_{m\mu}b_\mu$ being considered small in comparison. Substituting Eq. (5) into Eq. (3), we obtain with the given initial conditions the result

$$b_\mu(t)=\frac{(i\hbar)^{-1}H_{\mu m}e^{(i\Omega-\gamma_m/2)t}-e^{-\gamma_\mu t/2}}{i\Omega-\Gamma}, \tag{6}$$

where $\Omega=\omega-\omega_{m\mu}$ and $\Gamma=(\gamma_\mu-\gamma_m)/2$, and hence

$$|b_\mu(t)|^2=\left|\frac{H_{\mu m}}{\hbar}\right|^2\left[\frac{e^{-\gamma_m t}-e^{-\gamma_\mu t}-2e^{-(\gamma_\mu+\gamma_m)t/2}\cos\Omega t}{\Omega^2+\Gamma^2}\right]. \tag{7}$$

Equation (7) determines the probability that the atom will be found in the state $|\mu\rangle$ at time t if at $t=0$ it was in the state $|m\rangle$, and it is thus a function of time. Usually, what is required is the total probability that such a transition has occurred, which may be written as[9]

$$P_S=\gamma_\mu\int_0^\infty |b(t)|^2dt \tag{8}$$

and which, together with Eq. (7), gives the result

$$P_S=\left|\frac{2H_{\mu m}}{\hbar}\right|^2\frac{\gamma_\mu(\gamma_m+\gamma_\mu)}{4(\omega-\omega_{m\mu})^2\gamma_m\gamma_\mu+\gamma_m\gamma_\mu(\gamma_m+\gamma_\mu)^2}. \tag{9}$$

This may be compared with the expression for P_s which is valid for any level of the perturbation, viz.,[8,10]

$$P_S=\left|\frac{2H_{\mu m}}{\hbar}\right|^2\times\frac{\gamma_\mu(\gamma_m+\gamma_\mu)}{4(\omega-\omega_{m\mu})^2\gamma_m\gamma_\mu+(\gamma_m\gamma_\mu+|2H_{\mu m}/\hbar|^2)(\gamma_m+\gamma_\mu)^2}, \tag{10}$$

when it is seen that the results agree as expected for low levels of laser intensity. Equation (9) shows that at low power levels the linewidth of the transition is the sum of the natural lines of the upper and lower states. At higher power levels, Eq. (10) shows that P_s no longer increases linearly with the laser power, and that the resonance is broadened. Such variations will not affect the polarization of this particular transition, and it thus appears that the small-signal approximation should yield good results for the resultant polarization so determined from a number of overlapping Zeeman transitions, as shown in Fig. 1. There may be some variation in the polarization at high-power levels, especially for an asymmetrical position of the laser frequency with respect to the Zeeman levels, but the gross features deduced for the resultant polarization at low-power levels should persist at the higher values.

Considering now the general laser transition shown in Fig. 1, the probability amplitude of the state $|m=0\rangle$ may be written from Eq. (3) as

$$\dot{a}_0=(i\hbar)^{-1}[\langle 0|\mathcal{H}_e|1\rangle e^{i\omega_{01}t}b_1+\langle 0|\mathcal{H}_e|-1\rangle e^{i\omega_{0-1}t}b_{-1}]-a_0\gamma_m/2, \tag{11}$$

with similar equations for a_1 and a_{-1}. Similarly, for the lower μ levels, such as $|\mu=0\rangle$ we obtain

$$\dot{b}_0=(i\hbar)^{-1}[\langle 0|\mathcal{H}_e|-1\rangle e^{i\omega_{0-1}t}a_{-1}+\langle 0|\mathcal{H}_e|1\rangle e^{i\omega_{01}t}a_1]-b_0\gamma_\mu/2, \tag{12}$$

etc., for $\mu=2$, 1, -2, and -1. Figure 1 shows that the $\mu=0$ level is the only one on which both transitions corresponding to $\Delta M=\pm1$ terminate. Single transitions $\Delta M=+1$ terminate on levels $\mu=2$ and $\mu=1$, and transitions $\Delta M=-1$ terminate on levels $\mu=-2$ and $\mu=-1$. Such transitions correspond to equal and opposite frequency shifts from the degenerate case and will possess matrix elements which are numerically equivalent. They may thus be grouped in pairs in the summation of transitions, and essentially we need only consider the expression in Eq. (12) for b_0, since these other groups of transitions differ only by numerical constants, and can be incorporated later if necessary. The appropriate matrix elements for the transition $j\rightarrow j+1$ are given by[11]

$$(\alpha jm|\mathbf{r}|\alpha' j-1m\pm1)=\pm(\alpha j\vdots r\vdots\alpha' j-1)\times\tfrac{1}{2}[(j\mp m)(j\mp m-1)]^{1/2}(\mathbf{i}\pm i\mathbf{j}) \tag{13}$$

$$(\alpha jm|\mathbf{r}|\alpha' j-1m)=(\alpha j\vdots r\vdots\alpha' j-1)(j^2-m^2)\mathbf{k}.$$

As already intimated, in order to make the solution of Eqs. (11) and (12) tractable, and to obtain some physical interpretation, the assumption is made that the atom is at $t=0$ in a state corresponding to a coherent superposition of the states $|m\rangle$ with equal probabilities and that $b(0)=0$ for all μ levels. The perturbation due to the laser radiation is then assumed small so that the probability amplitudes a_m of the upper levels are determined by Eq. (5). Numerical constants corresponding to normalization will be omitted; this will not affect the results obtained. Substituting Eq. (5) into Eq. (12) and solving, we obtain

$$b_0(t)=(i\hbar)^{-1}\left[H_{0-1}\frac{e^{[i(\omega-\omega_{0-1})-\gamma_m/2]t}-e^{-\gamma_\mu t/2}}{i(\omega-\omega_{0-1})+\Gamma}+H_{01}\frac{e^{[i(\omega-\omega_{01})-\gamma_m/2]t}-e^{-\gamma_\mu t/2}}{i(\omega-\omega_{01})+\Gamma}\right]. \tag{14}$$

[9] P. Kusch and V. W. Hughes, *Handbuch der Physik*, edited by S. Flügge (Springer-Verlag, Berlin, 1959), Vol. 37, Part 1, pp. 1–172.

[10] W. R. Bennett, Jr., Phys. Rev. **126**, 580 (1962).

[11] E. U. Condon and G. H. Shortley, *The Theory of Atomic Spectra* (Cambridge University Press, New York, 1935), p. 63.

The matrix elements H_{0-1} and H_{01} in Eq. (14) are given by Eqs. (4) and (13), and will involve the intensity and polarization of the laser radiation. This builds up from the spontaneous emission of the specific photon types such as the left- and right-handed circular polarizations determined by such matrix elements, and which the laser cavity will accept. From these equations and the rotating wave approximation we deduce that

$$\langle \mu=0|H|m=\pm 1\rangle=\pm C_{\alpha j,\alpha' j-1}(1/\sqrt{2})(\mathbf{i}\pm i\mathbf{j})E/2. \quad (15)$$

Similar transitions to the $\mu=\pm 2$ levels and to the $\mu=\pm 1$ levels have the numerical constants $\sqrt{3}$ and $\sqrt{3}/\sqrt{2}$, respectively. Thus the oscillating electric dipoles $\mathbf{i}+i\mathbf{j}$ and $\mathbf{i}-i\mathbf{j}$ correspond to the emission of left- and right-handed circular polarization, respectively, and under the assumption of overlapping levels, coherent transitions may be summed to obtain the resultant polarization of the emission. With $\Omega=\omega-\omega_{0-1}=\omega_{01}-\omega=geH/2mc$, or the laser frequency symmetrical with respect to these transitions, Eqs. (14) and (15) give the result

$$b_0(t)=\frac{eE}{\hbar}\frac{1}{\sqrt{2}}e^{-\gamma_\mu t/2}\left[\frac{\mathbf{i}(\Omega e^{\Gamma t}\cos\Omega t-\Omega-\Gamma e^{\Gamma t}\sin\Omega t)+\mathbf{j}(\Gamma e^{\Gamma t}\cos\Omega t-\Gamma+\Omega e^{\Gamma t}\sin\Omega t)}{\Gamma^2+\Omega^2}\right]. \quad (16)$$

Equation (16) shows that the resultant polarization will be linear, and at some angle to the axes. For $\Omega=0$, or no applied magnetic field, the polarization is along the y axis, and as Ω increases it will rotate towards the x axis. The other transitions shown in Fig. 1 may be considered in an analogous way, and, for the axial magnetic field considered here, contain the same factor $f(\Omega,t,\Gamma)$ multiplied by the different numerical constants already given. Such numerical factors for the various transitions must be considered when the intensity of the over-all transition is required, but they will not affect the determination of the rotation of the plane of polarization in this particular case. Such conclusions only apply when the g factors of the states are equal; if this is not so, the problem becomes more complex. A similar reduction of Eq. (14) can be made with $\Omega_1=\omega-\omega_{0-1}$ and $\Omega_2=\omega_{01}-\omega$, or with the laser frequency not symmetrical with respect to the transitions. The resultant polarization is then elliptically polarized with parameters depending on the relative magnitudes of Ω_1 and Ω_2. We note from Eq. (16) that the direction of rotation of the electric vector changes when the magnetic field is reversed.

The probability amplitudes in Eq. (16) for polarizations in the x and y directions, given by the coefficients of $\mathbf{i}$ and $\mathbf{j}$, respectively, are functions of time. To proceed, we use Eq. (8) to determine the total transition probability separately for each of these polarizations. The results will correspond to the intensities I_x and I_y, and the rotation ϕ of the plane of polarization is given by

$$\tan\phi=E_x/E_y=(I_x/I_y)^{1/2}, \quad (17)$$

since the electric fields are coherent. From Eqs. (8) and (16) we thus obtain

$$\begin{aligned} I_x&=\frac{\gamma_\mu}{2}\left(\frac{eE}{\hbar}\right)^2\left[\frac{\tfrac{1}{2}\gamma_m(\Omega^2-\Gamma^2)-2\Omega^2\Gamma}{\gamma_m^2+4\Omega^2}+\frac{\Gamma^2+\Omega^2}{2\gamma_m}+\frac{\Omega^2}{\gamma_\mu}-\frac{2\Omega^2\gamma_m}{\Gamma_1^2+\Omega^2}\right](\Gamma^2+\Omega^2)^{-2},\\ I_y&=\frac{\gamma_\mu}{2}\left(\frac{eE}{\hbar}\right)^2\left[\frac{\tfrac{1}{2}\gamma_m(\Gamma^2-\Omega^2)+2\Omega^2\Gamma}{\gamma_m^2+4\Omega^2}+\frac{\Gamma^2+\Omega^2}{2\gamma_m}+\frac{\Gamma^2}{\gamma_\mu}-\frac{2\Gamma(\Gamma\Gamma_1+\Omega^2)}{\Gamma_1^2+\Omega^2}\right](\Gamma^2+\Omega^2)^{-2}, \end{aligned} \quad (18)$$

and hence

$$\tan^2\phi=\left[\frac{\tfrac{1}{2}\gamma_m(\Omega^2-\Gamma^2)-2\Omega^2\Gamma}{\gamma_m^2+4\Omega^2}+\frac{\Gamma^2+\Omega^2}{2\gamma_m}+\frac{\Omega^2}{\gamma_\mu}-\frac{2\Omega^2\gamma_m}{\Gamma_1^2+\Omega^2}\right]\left[\frac{\tfrac{1}{2}\gamma_m(\Gamma^2-\Omega^2)+2\Omega^2\Gamma}{\gamma_m^2+4\Omega^2}+\frac{\Gamma^2+\Omega^2}{2\gamma_m}+\frac{\Gamma^2}{\gamma_\mu}-\frac{2\Gamma(\Gamma\Gamma_1+\Omega^2)}{\Gamma_1^2+\Omega^2}\right]^{-1}, \quad (19)$$

where $\Gamma_1=(\gamma_\mu+\gamma_m)/2$. Equations (18) show that the total probability of the transition P_T, which is proportional to I_x+I_y, is given by

$$P_T=2\left(\frac{eE}{\hbar}\right)^2\frac{\gamma_\mu(\gamma_m+\gamma_\mu)}{4(\omega-\omega_{m\mu})^2\gamma_m\gamma_\mu+\gamma_m\gamma_\mu(\gamma_m+\gamma_\mu)^2}. \quad (20)$$

This result is the same as that given by Eq. (10) for the simple two-level system and indicates that the overlapping transitions can be regarded as a transition between composite levels, giving rise to various resultant polarizations depending on the magnetic field and laser frequency, but with an over-all transition probability similar to that for a simple two-level system. Equation (19) shows that $\phi=0$ when $\Omega=0$, or in zero magnetic field the radiation is polarized along the y direction. Also putting $\gamma_\mu=0$, as in studies of the polarization of resonance radiation, Eq. (19) gives

$$P=\frac{I_y-I_x}{I_y+I_x}=\frac{1-(\tau_m geH/mc)^2}{1+(\tau_m geH/mc)^2} \quad (21)$$

and

$$\tan\phi=\tau_m geH/mc, \quad (22)$$

where $\tau_m=1/\gamma_m$ is the lifetime of the upper levels of the transition.

It is interesting to note that Eqs. (21) and (22), which have been deduced as limiting cases of the perturbation treatment, can also be deduced from the result given by Eq. (157) of Ref. 4. Here Breit has deduced the probability amplitude for the emission of a particular photon type at a frequency ν_g. The result may be written as

$$c_g=K\sum_m \frac{f_{m\mu}g_{\mu m}e^{-i\omega t}}{i[\omega-\omega(m,\mu)]-\gamma_m/2}, \tag{23}$$

where $f_{m\mu}$ and $g_{\mu m}$ are the matrix elements for absorption and emission as determined here from Eqs. (13). For a magnetic field in the z direction Eq. (23) gives

$$c_g=Ke^{-i\omega t}\left[\frac{\mathbf{i}-i\mathbf{j}}{i\Omega-\gamma_m/2}-\frac{\mathbf{i}-i\mathbf{j}}{i\Omega+\gamma_m/2}\right], \tag{24}$$

and hence the intensities become

$$I_x\propto\frac{{\gamma_m}^2}{(\Gamma^2+\Omega^2)^2}, \quad I_y\propto\frac{4\Omega^2}{(\Gamma^2+\Omega^2)^2}. \tag{25}$$

Equations (25) give the same results as Eqs. (21) and (22) for the polarization P and rotation ϕ of the plane of polarization, and indicate the way in which the results on the depolarization of resonance radiation are analogous to those discussed here in connection with the highly monochromatic radiation involved in the laser. However, the final expressions for P and ϕ, obtained by integrating over the frequency widths of the spontaneous emission in resonance radiation studies, are given by[4]

$$P=P_0/[1+(\tau_m geH/mc)^2]; \quad \tan 2\phi=\tau_m geH/mc, \tag{26}$$

and hence differ from the results applicable to the laser. Taking $\gamma_m=10^7$ sec^{-1} and $\gamma_\mu=8\times10^7$ sec^{-1} as representative values for the 1.153-μ He-Ne transition,[10] the relation between ϕ and H in Eq. (19) is shown in Fig. 2. For comparison the values given by Eq. (26) are also shown in the figure. It is clear that large rotations of the plane of polarization, ranging up to 45° for magnetic fields between 0 and 1 G, may be expected. For negative values of H, ϕ becomes negative, and rotations of 90° are possible with ac magnetic fields.

b. Transverse Magnetic Field

This is discussed similarly using Eqs. (3), (4), and (5), together with the appropriate matrix elements from Eq. (13). The transitions involved together with the geometry considered are shown in Fig. 3. There are thus nine transitions with $\Delta M=0, \pm1$. Assuming that the laser frequency is again symmetrical with respect to the transitions, and that the g values are the same, then $\Omega=0$ for the π transitions which are polarized along the z axis, or the direction of the magnetic field. With the geometry shown in Fig. 3, the σ transitions are polarized along the x axis. All transitions with a given polarization must be summed coherently to determine the resultant polarization. Again in the small-signal approximation the probability amplitude for $b_0(t)$ is given by

$$b_0(t)=(i\hbar)^{-1}e^{-\gamma_\mu t/2}\left[H_{0-1}\frac{e^{(i\Omega+\Gamma)t}-1}{\Gamma+i\Omega}+H_{00}\frac{e^{\Gamma t}-1}{\Gamma}+H_{01}\frac{e^{(\Gamma-i\Omega)t}-1}{\Gamma-i\Omega}\right], \tag{27}$$

with similar equations for $\mu=2$, 1, -1, and -2. Inserting the matrix elements from Eq. (13) we obtain

$$b_0(t)=\frac{eE}{2i\hbar}e^{-\gamma_\mu t/2}\left\{\frac{\mathbf{i}}{\sqrt{2}}\left[\frac{2i(\Omega e^{\Gamma t}\cos\Omega t-\Omega-\Gamma e^{\Gamma t}\sin\Omega t)}{\Gamma^2+\Omega^2}\right]+\frac{\mathbf{k}2e^{\Gamma t}-1}{\Gamma}\right\}. \tag{28}$$

As before, the polarizations in the $\mathbf{i}$ and $\mathbf{k}$ directions are now dealt with independently in forming the expression for the total transition probability P_s given by Eq. (8). From Eq. (28) and similar equations for $b_2(t)$, etc., the resultant intensities in the x and z directions are given by

$$I_x=(1/\sqrt{2}+\sqrt{3}/\sqrt{2}+\sqrt{3})^2\gamma_\mu\left(\frac{eE}{2\hbar}\right)^2 4\left[\frac{\tfrac{1}{2}\gamma_m(\Omega^2-\Gamma^2)-2\Omega^2\Gamma}{{\gamma_m}^2+4\Omega^2}+\frac{\Gamma^2+\Omega^2}{2\gamma_m}+\frac{\Omega^2}{\gamma_\mu}-\frac{2\Omega^2\gamma_m}{{\Gamma_1}^2+\Omega^2}\right](\Gamma^2+\Omega^2)^{-2}, \tag{29}$$

$$I_z=(2+2\sqrt{3})^2\left(\frac{eE}{2\hbar}\right)^2\frac{4\gamma_\mu}{\gamma_m\gamma_\mu(\gamma_m+\gamma_\mu)},$$

and hence

$$\tan^2\phi=\left[\frac{(1/\sqrt{2})+(\sqrt{3}/\sqrt{2})+\sqrt{3}}{\Gamma^2+\Omega^2}\right]^2\left[\frac{\tfrac{1}{2}\gamma_m(\Omega^2-\Gamma^2)-2\Omega^2\Gamma}{{\gamma_m}^2+4\Omega^2}+\frac{\Gamma^2+\Omega^2}{2\gamma_m}+\frac{\Omega^2}{\gamma_\mu}-\frac{2\Omega^2\gamma_m}{{\Gamma_1}^2+\Omega^2}\right](2+2\sqrt{3})^{-2}[\gamma_m\gamma_\mu(\gamma_m+\gamma_\mu)]. \tag{30}$$

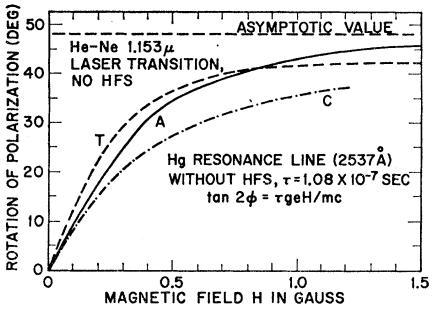

FIG. 2. Theoretical results for the rotation of the polarization of the laser output with magnetic field: Curve A—axial magnetic field; curve B—transverse magnetic field; curve C—classical result for the rotation of the plane of maximum polarization of the resonance line of Hg.

The laser radiation is thus polarized along the z direction in zero magnetic field, but on applying a magnetic field along this direction an orthogonal polarization in the x direction appears corresponding to a rotation of the plane of polarization. With $\gamma_\mu=0$ in Eq. (29), results similar to those given by Eqs. (21) and (22) are obtained. These, however, are not exactly identical with those for the axial magnetic field. This is associated with the requirement that although the polarization in zero magnetic field must be the same, irrespective of the initial direction of magnetic field; the manner in which this polarization is approached will depend on this direction. The variation of the angle of rotation of the polarization with magnetic field is also shown in Fig. 2 for $\gamma_m=10^7$ sec^{-1} and $\gamma_\mu=8\times10^7$ sec^{-1}. It is seen that the rotations are similar to those for the axial magnetic field, though the two curves differ in shape.

3. EXPERIMENTAL RESULTS

a. General Considerations and dc Magnetic Fields

A relatively short He-Ne laser of the planar or internal optics type was constructed for use in the investigations. This operated on the 1.153-μ transition with a reflector spacing of some 28.3 cm, which gave a frequency separation between axial modes of 530 Mc/sec. Such a frequency separation was sufficiently large as to allow operation in a single axial mode under most conditions, except at high levels of rf excitation of the discharge, when difficulties were encountered in single mode operation. The bore of the laser tube was 3 mm with the discharge 15 cm long and was excited by an rf source at 52.5 Mc/sec. Axial magnetic fields were applied with a solenoid 20 cm long and diameter 4.5 cm, wound with two layers of wire at 7 turns per cm, and placed around the laser tube. The solenoid was surrounded by a number of layers of magnetic shielding material in order to shield the laser from the earth's magnetic field or other stray fields, and also to shield the laser supporting structure, which consisted partly of magnetic materials, from stray fields originating in the solenoid, and which might result in inadvertent tuning effects. The stray magnetic field inside the solenoid could not be measured after its assembly around the laser, but measurements in its proximity indicated that a residual magnetic field around 0.1 G might exist around the laser tube. This is partly due to the necessity for holes in the shielding where the laser tube leaves the solenoid.

The rotation of the plane of polarization of the laser output with small magnetic fields, as predicted by the theory, has been observed by several methods. Under carefully controlled conditions, small dc magnetic fields were applied to the laser and the rotation of the plane of polarization observed. Because of thermal drifts in the laser during the time interval involved in such measurements, the results obtained vary somewhat in degree, though they are consistent as regards a definite rotation. To avoid these changes during the time of observation, a sawtooth waveform of magnetic field was applied to the laser. The resulting polarization changes were then observed by passing the laser radiation through an analyzer orientated at various angles, with the signal resulting from the sweep detected by a photomultiplier and displayed on an oscilloscope. Otherwise, small ac magnetic fields have been applied to the laser and the rotation of the plane of polarization converted into amplitude modulation by passing the beam through an analyzer. All these methods have been used and are described below together with the results, which corroborate each other.

As mentioned above, the present laser arrangement is not sufficiently precise and stable enough against thermal and other disturbances to yield the detailed shape of the rotation of polarization versus dc magnetic field. Small temperature changes appear to cause the laser to drift during the period of measurement. It will

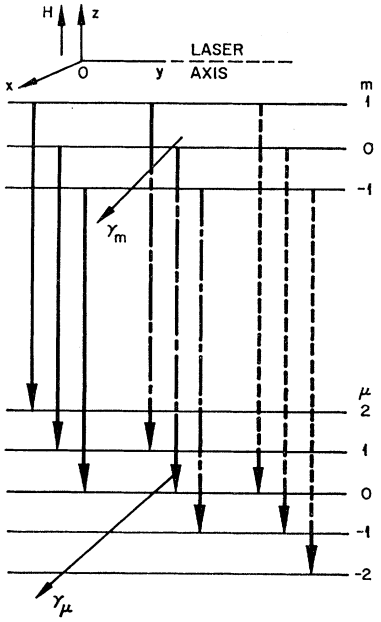

FIG. 3. Overlapping Zeeman levels, decay constants, and transitions involved for a transverse magnetic field in the z direction on the laser.

be recalled that the laser frequency should remain symmetrical with respect to the Zeeman transitions, or should remain at the center of the Doppler distribution. However, from a number of such measurements taken over a period of time, it is established that a rotation of the polarization of approximately 45° is observed as the magnetic field is increased from zero up to a fraction of a gauss. The amount of rotation seems to depend on the intensity of the laser oscillation, decreasing as the intensity is reduced by decreasing the rf excitation of the laser, or by slightly detuning the reflectors. Also the amount of rotation for a given magnetic field is a function of the detuning of the laser resonator from the Doppler line center, the rotation decreasing and eventually disappearing as the resonance is moved away from the line center. Figure 4 shows two typical curves of rotation versus magnetic field. Curve A applies for an rf excitation of 25 W, and curve B for 20 W, with the reflectors peaked for maximum output in each case. The laser output powers for curves A and B were in the ratio of 1.45:1. It is apparent that the rotation occurs at much lower values of magnetic field for the oscillation of greatest intensity. Since the curves are not symmetrical with respect to zero magnetic field, or more correctly zero current in the solenoid, it can be concluded that a residual magnetic field is present. A total rotation of 90° could also be obtained in curve B, if the magnetic field was increased sufficiently. Because of the difficulties in doing these measurements, it is difficult to say whether the nonlinear regions of the curves are real or due to variations in the laser operation during the measurements.

Figures 5(a)–(d) show the results obtained by applying a sawtooth variation of magnetic field in the solenoid and passing the laser radiation through an analyzer kept fixed at various angles to the polarization in zero magnetic field. The resulting signals are detected by a photomultiplier and displayed on an oscilloscope. In Fig. 5(a), the sawtooth current wave form applied to the solenoid is shown in the lower trace, the frequency being

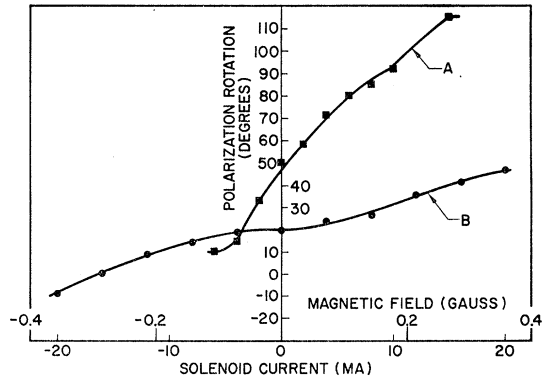

FIG. 4. Experimental results on the rotation of polarization with an applied axial magnetic field. Curve A—rf drive 25 W, laser intensity, 1.45 (relative units); curve B—rf drive, 20 W, laser intensity 1.0 (relative units).

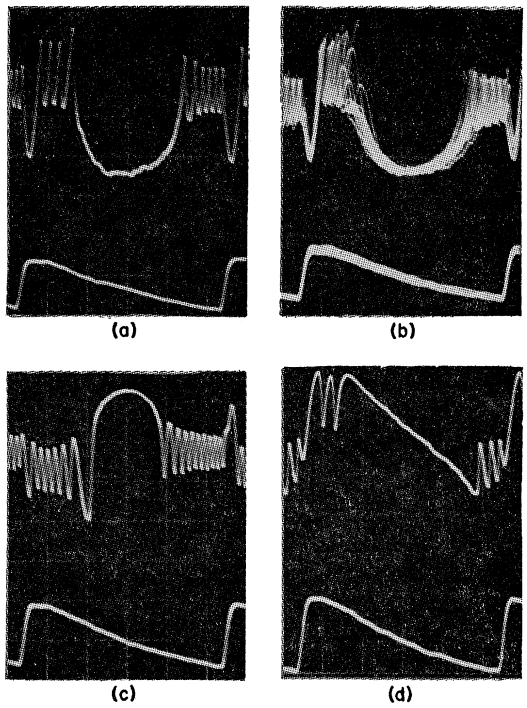

FIG. 5. Sawtooth waveform of magnetic field applied axially on the laser (lower trace of all figures). Frequency 400 cps, 0.36 G peak value. Sweep 0.5 msec/cm. (a) Analyzer along E vector in zero magnetic field. (b) Multiple sweep showing general level of laser stability. (c) Analyzer at 90° to E vector in zero field. (d) Analyzer at 45° to E vector in zero field. Note the circularly polarized beats either side of each response, showing the magnetic field at which coherence is lost.

400 cps, the current 40 mA peak-to-peak ($H \approx \pm 0.36$-G peak), and the sweep 0.5 msec/cm. Here the analyzer is oriented so as to pass the linear polarization of the laser radiation in zero magnetic field. This position corresponds to the center of the traces, the minimum in the upper signal trace corresponding to a maximum signal. As the magnetic field is swept through zero, the polarization rotates and the signal decreases as $\cos^2\phi$, giving the U-shaped curve at the center of the upper trace, with the polarization remaining linear over this region. The oscillations which appear on either side when the magnetic field increases further are due to low-frequency beats between oscillations which are circularly polarized, and which appear when the coherence between the Zeeman levels breaks down and the normal circularly polarized transitions occur. We note that a narrower U-curve appears also on the return sweep of the sawtooth. Figure 5(a) was taken with a single sweep of the sawtooth magnetic field; in comparison, Fig. 5(b) shows the results obtained with a multiple sweep and indicates that drifts and other disturbances of the laser are present as inferred above. In Fig. 5(c) the analyzer has been rotated so that it is at 90° to the polarization of the laser radiation in zero magnetic field. The maximum of the inverted U-curve

now corresponds to zero signal; and, as the magnetic field sweeps through zero, the signal increases as $\sin^2\phi$, giving the response shown; the oscillations on either side are again due to circularly polarized oscillations at the higher magnetic fields. The upper trace of Fig. 5(d) shows the signal obtained when the analyzer is orientated at 45° with respect to the polarization in zero magnetic field, and the sawtooth variation of magnetic field is applied. Here a relatively linear change in the signal, which is proportional to $\cos^2\phi$, occurs in the region of $\phi=45°$. Other types of response can be similarly obtained for other orientations of the analyzer. These results illustrate very clearly the rotation of the plane of polarization which occurs for small magnetic fields, when the cavity resonance is symmetrical with respect to the transitions. By applying a pressure along the laser axis in as symmetrical a manner as possible at the present stage, such responses as those in Fig. 5(c) have been found to appear and disappear at periodic intervals presumably as the cavity is tuned through the line center. Such phenomena require a more precise investigation, but they represent a potential method for tuning the laser to the center of the Doppler distribution.

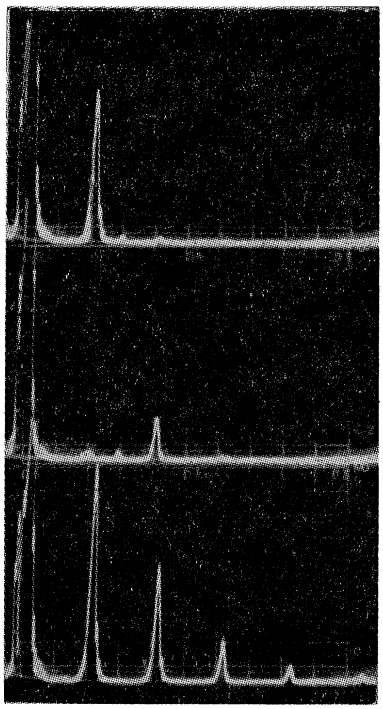

FIG. 6. Modulation due to ac magnetic fields along axis of laser and periodic rotation of polarization. Magnetic field 0.4 G peak, frequency 10 kc/sec. Spectrum analyzer sweep 5 kc/sec/cm, with zero frequency on the left. Upper—analyzer at 45° to E vector in zero field, fundamental component. Middle—analyzer along E vector in zero field; second harmonic produced. Lower—ac magnetic field increased to 1.2 G peak, more harmonic frequency components appear. All components are linearly polarized.

b. ac Magnetic Fields

In these investigations, the plane of polarization is made to rotate in a periodic way by applying small ac magnetic fields. The periodic rotation is then passed through an analyzer and converted into amplitude modulation, the spectrum of which can be displayed with a photomultiplier and spectrum analyzer. The rotation thus occurs in a short time interval and eliminates thermal and other effects on the laser. Assuming that operation occurs on the linear portion of the curve of rotation ϕ against magnetic field H, we may write

$$\phi=kH=kH_0\sin\omega_m t, \tag{31}$$

where k is a constant slope factor, H_0 is the amplitude of the ac magnetic field, and ω_m is its frequency. The electric field due to the laser, and which is passed by the analyzer, is then given by

$$E=E_0\cos\omega t\cos(kH_0\sin\omega_m t). \tag{32}$$

Hence, using the expansion

$$\cos(k\sin\omega_m t)=\sum_{n=-\infty}^{\infty}J_n(kH_0)\cos n\omega_m t,$$

where J_n is the Bessel function of order n, the photomultiplier output is determined by

$$S\propto[E_0\cos\omega t\sum_{n=-\infty}^{\infty}J_n(kH_0)\cos n\omega_m t]^2. \tag{33}$$

The nonlinear regions of ϕ versus H can be dealt with similarly by an appropriate series expansion involving higher powers of H. From Eq. (33) and the relation $J_{-n}=(-1)^nJ_n$ we see that all odd harmonics, including the fundamental, will be zero, and only even harmonics will appear in the detected signal displayed on the spectrum analyzer. Odd harmonics will appear, however, when H_0 is increased so that nonlinear regions of the curve are used. Similarly, if the analyzer is at an angle ϕ_0 to the polarization in zero magnetic field, we may write

$$\phi=\phi_0+kH_0\sin\omega_m t, \tag{34}$$

and a similar analysis shows that the fundamental frequency ω_m and its harmonics will appear in the detected signal. ϕ_0 will usually be 45° in the experiments, corresponding to the maximum rotation of the plane of polarization obtained for one direction of the dc magnetic field.

Figure 6 shows a harmonic spectrum of the modulation of the laser beam produced by the periodic rotation of the plane of polarization due to an ac magnetic field. The modulation or frequency of the ac magnetic field was 10 kc/sec, and the spectrum analyzer sweep 5 kc/sec/cm. For the top and center traces, the ac magnetic field was 0.4 G peak. The center trace shows the second harmonic produced when the analyzer is oriented in the direction of polarization in zero magnetic field. The amplitude is small due to the order of the Bessel function, and the result is in agreement with that predicted by Eq. (33). In the top trace, the analyzer is at 45° to the polarization in zero magnetic field, thus producing maximum modulation at the fundamental frequency. For the lower trace, the ac magnetic field was increased to 1.2 G peak with the analyzer oriented

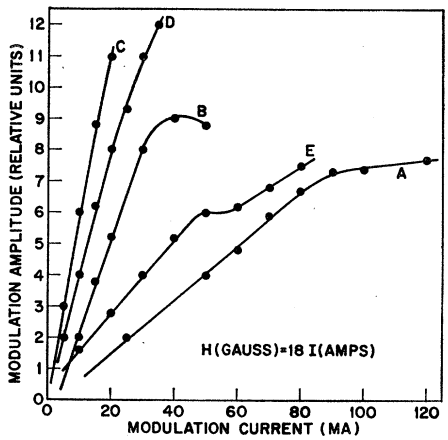

FIG. 7. Modulation amplitude vs amplitude of ac magnetic field for various levels of rf excitation. Curve A—rf 15 W, $I=2.25$; curve B—rf 20 W, $I=2.9$; curve C—rf 25 W, $I=3.9$; curve D—rf 30 W, $I=3.9$; curve E—rf 35 W, $I=4.0$. I=photomultiplier dc current with no modulation (amps$\times 10^7$).

as in the center trace. It is seen that additional harmonics appear as the amplitude of the ac magnetic field is increased. This is again in agreement with Eq. (33), but with the additional and possibly more pronounced effects of the nonlinear regions of the ϕ versus H curve as the amplitude of the ac field is increased. The higher harmonics shown in the lower trace are also linearly polarized, and they disappear when the analyzer is removed, showing that the modulation is due to a periodic rotation of the plane of polarization of the laser radiation by the ac magnetic field.

The result shown in Fig. 4 that a smaller rotation for the same magnetic field occurs for lower values of laser intensity is also substantiated by the modulation results. Figure 7 shows the modulation amplitude, as in the upper trace of Fig. 6, as a function of the amplitude of the ac magnetic field for various levels of rf excitation. The variation with rf power level is evident, the modulation due to the rotation of the plane of polarization, peaking around a relative rf excitation of 25 W. The modulation amplitude decreases as the rf excitation increases beyond this value, although the laser intensity, as indicated by the dc current of the photomultiplier, remains the same. Since the modulation amplitude for a given ac magnetic field depends on both the amount of rotation of the plane of polarization and the laser intensity, a more useful comparison of how the modulation amplitude changes with rf excitation is to normalize the results with respect to intensity. The results are shown in the following table:

Relative level of rf power (W)	Modulation amplitude (relative units) normalized to dc intensity
15	0.252
20	0.635
25	1.000
30	0.728
35	0.257

Again a definite dependence on rf power level is present.

A similar decrease in the modulation amplitude also took place when the rf excitation and the ac magnetic field were kept constant, but the laser output was decreased by detuning the cavity. Exceptions arose when the cavity tuning was near optimum, when the modulation amplitude was relatively unaffected by small changes in tuning, but it did decrease drastically for tuning conditions far from optimum. Since in the present laser the angular and translational adjustments are not independent, it is difficult to say whether optimum modulation amplitude is due to a better centering on the Doppler distribution, or to improved angular alignment of the reflectors. However, it has been observed that when more than one axial mode is oscillating the rotation does not occur, in general, with the present laser.

Some idea of the time constant of the rotation process is obtained by studying the modulation amplitude as a function of the frequency of the ac magnetic field, with the amplitude of the field kept constant. Figure 8 shows the decrease in modulation amplitude which is observed as the frequency of the ac magnetic field is increased beyond a few kc/sec. This frequency dependence appeared to be independent of the rf excitation as far as we could determine. The modulation amplitude at higher ac frequencies may be increased by increasing the amplitude of the ac magnetic field. However, the ultimate value before distortion occurs is smaller than the modulation amplitude at lower frequencies.

c. Harmonic Effects

In addition to modulation at the fundamental frequency of the ac magnetic field, as produced by the rotation of the plane of polarization and the analyzer, harmonic components are produced when the amplitude of the ac magnetic is increased, and in particular when it is large enough so that excursions into the nonlinear regions of the ϕ versus H curve occur. Figures 9(a) and (b) illustrate the modulation as a function of the amplitude of the ac magnetic field. The upper traces in both figures correspond to conditions for maximum amplitude of the fundamental component shown on the trace just before distortion occurs. The modulation frequency of the ac magnetic field is 10 kc/sec, the spectrum analyzer

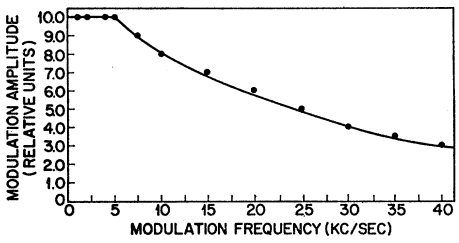

FIG. 8. Amplitude of fundamental component of modulation versus frequency of the ac magnetic field. The amplitude of the ac magnetic field is kept constant.

sweep 5 kc/sec/cm, and the analyzer is at 45° to the polarization in zero magnetic field. Figures 9(a) and (b) differ because of a slight difference in cavity tuning. The modulating magnetic fields used in Fig. 9(a) were 0.4, 0.5, and 1.0 G from the top to the bottom trace. Similarly, in Fig. 9(b) the fields were 0.8, 1.4, and 2.5 G, respectively. It is interesting to note that for the larger values of ac magnetic field, the modulation shows apparent subharmonic components at 5 kc/sec, as seen in the lower trace of Fig. 9(a), and at other times it shows components which do not seem to be harmonically related to the fundamental frequency. The harmonic components at multiples of 10 kc/sec, as in the middle trace of Fig. 9(b), are always linearly polarized. When components occur at 5-kc/sec intervals, some may be linearly polarized, but others have elliptical and circular polarizations. As the modulating magnetic field is increased further, more and more of the 5-kc/sec components become circularly polarized. For sufficiently high magnetic fields, all the harmonics seen on the spectrum analyzer are circularly polarized or arise from beats between laser oscillations which are circularly polarized. Two processes are involved here; one is the modulation produced by the periodic rotation of the plane of polarization and the analyzer, the other is the low-frequency beat phenomena[1] produced at larger magnetic fields when the coherence between the transitions breaks down.

The wave forms of the modulated output under these conditions are of interest and are shown in Figs. 10(a) and (b). The upper traces in these figures shows the frequency spectrum, and the lower oscilloscope traces

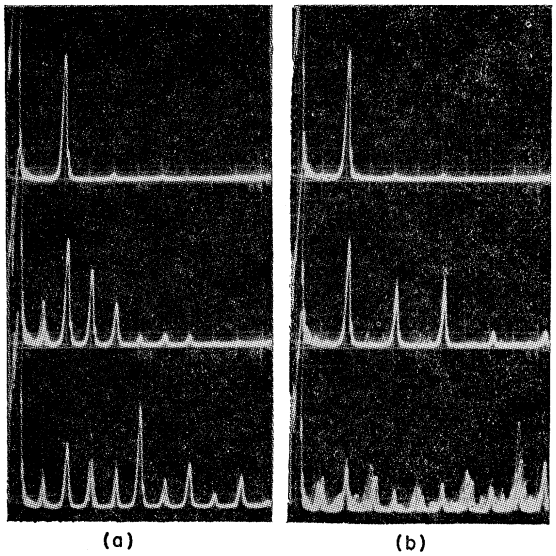

FIG. 9. Subharmonic phenomena at higher amplitudes of the ac magnetic field. (a) Upper—fundamental component at 10 kc/sec, amplitude 0.4 G. Middle and lower traces—components at 5 kc/sec appear—amplitudes of ac magnetic field 0.5 and 1 G, respectively. (b) Similar results—amplitudes of ac field 0.8, 1.4, and 2.5 G from upper to lower traces. Circularly polarized components appear.

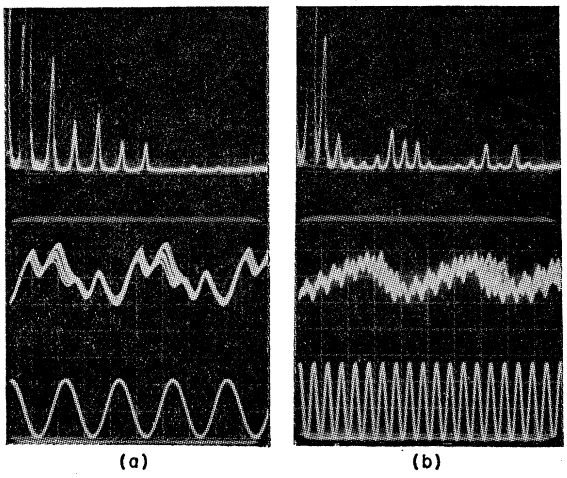

FIG. 10. Wave forms of the ac magnetic field and the modulated laser beam for ac magnetic along axis of the laser: (a) frequency 10 kc/sec, 2 G peak; (b) frequency 20 kc/sec, 3 G peak.

the wave form of the laser modulation after the analyzer together with the wave form of the ac magnetic field applied to the laser. In Fig. 10(a), the ac frequency is 10 kc/sec, the spectrum analyzer sweep 5 kc/sec/cm, the oscilloscope sweep 50 μsec/cm, and the ac magnetic field 2 G peak. The spectrum again shows frequencies at 5-kc/sec intervals; the first and third components of the spectrum are elliptically polarized and have the same dependence on analyzer orientation. The second and fourth components are very nearly circularly polarized. Corresponding to this spectrum, the modulation waveform indicates frequency components at 5 kc/sec and at 20 kc/sec. In Fig. 10(b), the ac frequency of the magnetic field is 20 kc/sec, the spectrum analyzer sweep 5 kc/sec/cm, the oscilloscope sweep 100 μsec/sec, and the ac magnetic field 3-G peak. An even greater number of "subharmonics" around 2.5 kc/sec is apparent in the spectrum. All the frequency components are circularly polarized, showing that the magnetic field is sufficiently large to produce low-frequency beats with the circular polarizaton due the axial magnetic field. The wave form of the laser modulation is even more complex. Two distinct time variations are apparent, one is the slow variation corresponding to a frequency around 2.5 kc/sec, superposed on this is a rapid fluctuation at some 40 kc/sec, which is the second harmonic of the fundamental frequency 20 kc/sec.

d. Additional Coherence Effects

The planar laser used in the work, described in Ref. 1, had a length of 125 cm and used a discharge tube with a bore of 1.5 cm. To obtain the circularly polarized low-frequency beats from Zeeman transitions, separated beyond their natural linewidths, it was necessary to increase the axial magnetic field used to a value around 10 G. This is an order-of-magnitude estimate since there was some variation in the field inside the solenoid due

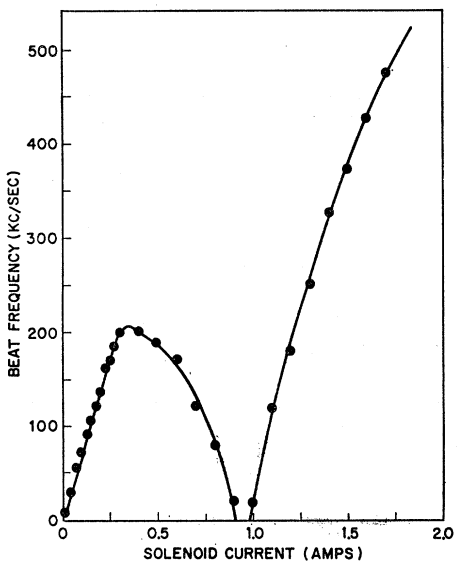

FIG. 11. Axial magnetic field—beat frequency between circularly polarized oscillations versus dc magnetic field. Note the null region where such beats disappear and coherence effects again occur.

to the length of discharge required for oscillation. However, in the present short laser with a 3-mm bore, the low-frequency beats appear at much lower values of magnetic fields. As the magnetic field is increased, the beat frequency between the circularly polarized oscillations increases to a maximum, then returns to zero again, after which it increases without any further reversals. The effect is shown in Fig. 11, which depicts a typical curve obtained. The shape of the curve remains essentially unchanged as the rf power and cavity tuning are varied, but the null point moves over a wide range. At very low values of rf drive, and hence low laser intensities, the effect is not observed.

At the null point, which in Fig. 11 corresponds to a magnetic field of 16 G, the low-frequency beats disappear, but the dc output due to the laser oscillation is unchanged. Furthermore, the output again becomes linearly polarized in the null region but is circularly polarized on either side of this position. This linearly polarized region, where the axial magnetic field apparently is such that the states should be separated, is evidence of an additional coherence which is imparted to the states where the null occurs. Some tentative explanation of this can be given from double-resonance studies on the laser,[12] as the rf excitation produces oscillating magnetic fields around the laser axis. The coherence at the null point in Fig. 11 is similar to that discussed for a near-zero magnetic field, and a similar rotation of the plane of polarization for small changes in magnetic field around this position has been observed. Because of thermal drifts due to the relatively large currents in the solenoid, no dc characteristics similar to those in Fig. 4 were taken, but the rotation was verified and appeared to be similar in magnitude. Also a small ac magnetic field was superimposed on the dc magnetic field required for the null, and modulation phenomena similar to those described above were observed. Figs. 12(a) and (b) depict the results obtained. Here a modulation frequency of 10 kc/sec was used again, the spectrum analyzer sweep is 5 kc/sec/cm, and the null region where the low-frequency beats disappear occurred here at dc magnetic fields extending from 7.03 to 7.39 G. Referring first to Fig. 12(a), the following conditions apply: Upper trace—no ac magnetic field, but dc magnetic field, 6.4 G. Usual circularly polarized low-frequency beat is present. Middle trace—no ac magnetic field but dc field of 6.95 G. Low-frequency beat approaching the null, and it has become weak and noisy but is still due to circularly polarized modes. Lower trace—ac magnetic field 0.267 G, dc magnetic field, 7.21 G. No beat seen unless the ac field is applied, when the resulting small linearly polarized modulation signal appears as shown. Figure 12(b) upper trace—same conditions, except ac field increased to 0.71 G. Modulation signal due to rotation of the plane of polarization in-

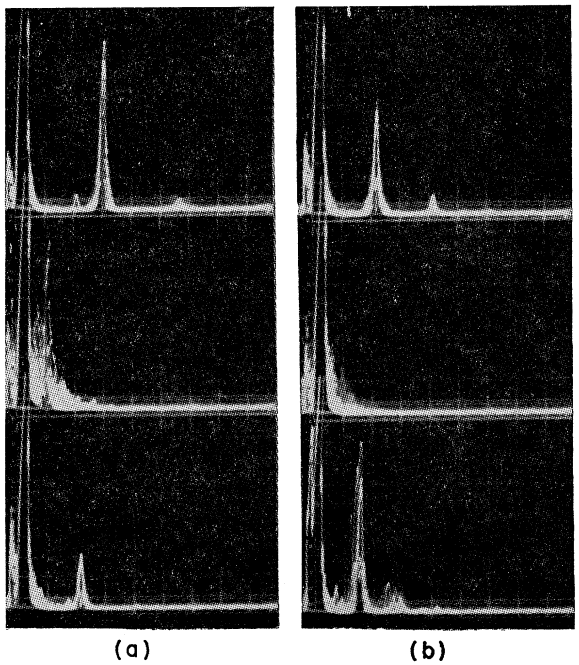

FIG. 12. Low-frequency beats between circularly polarized oscillations, and modulation effects due to rotations of the linear polarization by ac magnetic fields in the null region of Fig. 11. (a) Phenomena on the low side of the null. (b) Phenomena increasing to values of dc magnetic field above the null as discussed in the text.

[12] Double-resonance studies applicable to the laser, and involving the simultaneous action of optical transitions and rf perturbations between the Zeeman sublevels, show that additional coherence effects occur where the levels cross in the effective term diagram for such a system. W. Culshaw, Phys. Rev. **135**, A316 (1964). See also J. N. Dodd and G. W. Series, Proc. Roy. Soc. (London)**A263**, 353 (1961).

creases, still linearly polarized. Middle trace—ac field turned off, dc magnetic field increased to 7.48 G. Low-frequency beat is reappearing; it is weak and noisy at first but is circularly polarized. Lower trace—ac magnetic field zero, dc magnetic field 7.65 G. Usual low-frequency beats due to oscillations of opposite circular polarization are clearly seen. These results are of great interest in their own right, and in addition they lend confirmation to the results obtained in the rotation of the plane of polarization in near-zero magnetic fields.

4. CONCLUSIONS

The experimental results show that a rotation of the plane of polarization of the laser output occurs on applying a dc magnetic field and increasing it from zero to a fraction of a gauss. The rotation for a given value of magnetic field is much more pronounced at higher levels of rf excitation of the discharge and appears to be quite small when the laser is operated near threshold. The observed rotation also depends on the tuning of the laser cavity. Such measurements require accurate control of small magnetic fields and the elimination of random changes in stray magnetic fields or in the residual magnetization of the laser structure. Mechanical stability, precise tuning, and freedom from thermal drifts within the order of a natural linewidth are apparently required. Further quantitative measurements necessitate an improved laser design, but we can conclude that a rotation of approximately 45° occurs as predicted by theory, and at magnetic fields generally less than 0.5 G. The effect occurs consistently under proper operating conditions, i.e., a relatively high level of laser oscillation, and tuning of the cavity resonance to the proximity of the line center. Conversely, when the cavity resonance is removed from the line center, or when more than one axial mode is oscillating in our laser, then only a very small rotation, or none at all is observed. The criterion presently employed for proximity to the line center was a maximum output in a single mode. Effects due to inadvertent mechanical tuning of the laser cavity by changes in stray fields as the field in the solenoid is changed are precluded by the modulation results, especially those at the null point in Fig. 11 of the low-frequency beat, where both dc and ac magnetic fields are applied. The ac magnetic field is then but a small fraction of the dc field and is unlikely to effect the general level of stray magnetic field. Furthermore, the modulation is due to a rotation of the plane of polarization, as evidenced by its disappearance when the analyzer is removed.

Some variation of the rotation with rf excitation, or laser output, can be expected due to repopulation of the upper levels involved in the transition, and also because of line-broadening effects and variations in γ_m and γ_μ. The large effect which is observed, including the very small rotation at low levels of rf excitation is, however, not understood at present, particularly since the theory which predicted the rotation uses a small-signal approximation. Further investigations are required, including the use of a dc discharge to avoid any complications due to rf magnetic fields around the atoms. The excitation and saturation processes within the laser cavity also must be considered by methods similar to those used by Lamb in his theory of the optical maser.[13] However, the assumption of a coherent excitation with equal probabilities for the overlapping Zeeman levels of the neon atoms seems reasonable at present, particularly since the polarization at low levels of rf excitation is generally linear at small magnetic fields, indicating a coherent superposition of the transitions.

The fundamental and harmonic frequencies shown in Fig. 6 substantiate the theory of modulation due to a periodic rotation of the polarization of the laser output. Those in Figs. 9(a) and (b), which indicate subharmonic components, are not entirely explained. Two phenomena are present here, however, the production of modulation and harmonics due to the rotation of the linear polarization, and the appearance of circularly polarized oscillations at the extremes of the ac magnetic field, where the field is verying less rapidly and the states no longer overlap. Figure 8 shows that the amplitude of the fundamental component decreases as the frequency of the ac magnetic field increases, and becomes quite small at frequencies above 50 kc/sec. For a peak value of the ac field of 0.2 G, the precession rate of the atoms is about 300 kc/sec, which is much larger than these values of ω_m, and hence would not account for the decrease in modulation due to the periodic rotation of the polarization. Further substantiation of this is given by similar investigations in the null region shown in Fig. 11, where a similar decrease was also observed. Here the dc magnetic field is about 10 G, giving a much greater rate of atomic precession. The quality factor Q of the laser cavity could be as high as 10^8, giving a response width of 1 Mc/sec at the laser frequency, which again is high compared with the modulating frequencies ω_m. However, the rate of rotation of the polarization which the atom may emit is given by

$$d\phi/dt = k\omega_m H_0 \cos\omega_m t, \tag{35}$$

and thus increases with ω_m and H_0. The rate $d\phi/dt$ is thus a maximum when $\omega_m t = n\pi$, and zero when $\omega_m t = (2n+1)\pi/2$, which regions correspond, respectively, to those in which a rotation of the polarization occurs, and where the circularly polarized beats occur. Hence it may be that the build up of oscillations in the cavity is not rapid enough to follow the rotating polarization at the higher values of ω_m and H_0, which would explain the decrease in modulation amplitude shown in Fig. 8, and also the predominance of circularly polarized components at the higher values of H_0. The null region in Fig. 11, where similar results with ac magnetic fields

[13] W. E. Lamb, Jr., Phys. Rev. **134**, A1429 (1964).

are obtained, may well be associated with double-resonance phenomena,[12] in which levels can cross at values of dc magnetic field which differ from zero. To substantiate this, more appropriate geometries must be used to study the phenomena, which is of great interest.[14]

Finally, with increased precision the results described may be applied to studies of the lifetimes of the states involved in the laser, including the variation with laser geometry, intensity, and gas pressure. Studies of such processes involving coherent excitation and induced emission processes from overlapping atomic levels, and the interchange of the resulting polarization and energy with the laser cavity, are of fundamental importance in understanding the quantum electrodynamics of lasers. The results are also pertinent to investigations involving the complete ensemble of atoms corresponding to the Doppler distribution of frequencies which may be emitted by the moving atoms. Rotations of the linear polarization in near-zero magnetic fields are generally observed only when the laser cavity is tuned to the proximity of the center of the Doppler distribution, corresponding to a symmetrical disposition with respect to the atomic transitions, or to the use of atoms with near-zero velocities. The polarization also appears to remain linear for a larger variation of the dc magnetic field, the closer it is to the line center. Such observations indicate the use of the phenomena for tuning the laser to the center of the Doppler distribution. For resonances of the laser cavity which are removed from this position, atoms with a finite velocity must be used to obtain frequencies which are resonant with the cavity. The frequencies corresponding to the atomic transitions do not change with velocity, but only the apparent frequency with which the photon is emitted. The cavity resonant frequency ω will be such that the transition probabilities for the various overlapping transitions, involving the velocity of the atom, are equal. Since the atomic transition frequencies ω_{0-1} and ω_{01}, cf. Eq. (14), are different, they are affected to a different degree by the velocity of the atom, which means that the cavity resonance now becomes asymmetrical with respect to them. This would account for the various degrees of elliptical polarization which are observed, and for the decrease in the rotation of polarization with increasing departure of the cavity resonance from the center of the Doppler distribution.

[14] *Note added in proof.* An extension of Lamb's theory of the optical maser (Ref. 13) to cricularly polarized transitions, and to the coherence properties at small values of magnetic field, shows that a second coherence region as in Fig. 11 can occur even with dc magnetic fields. It thus appears that double resonance effects are not necessary for the explanation of the phenomena. This later work will be dealt with in another paper.

ACKNOWLEDGMENTS

We express our appreciation of the valuable efforts of L. B. Fowles and W. Proskauer on the construction and operation of the short planar laser which was used in the experiments.

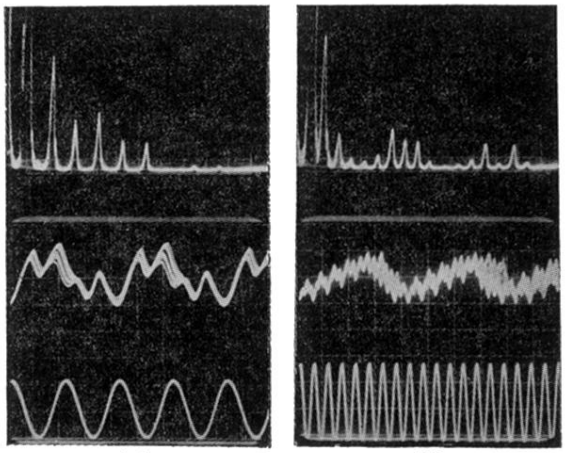

FIG. 10. Wave forms of the ac magnetic field and the modulated laser beam for ac magnetic along axis of the laser: (a) frequency 10 kc/sec, 2 G peak; (b) frequency 20 kc/sec, 3 G peak.

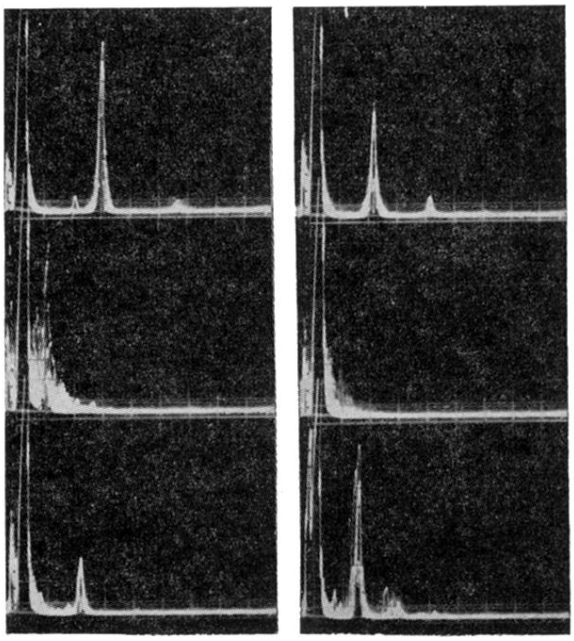

FIG. 12. Low-frequency beats between circularly polarized oscillations, and modulation effects due to rotations of the linear polarization by ac magnetic fields in the null region of Fig. 11. (a) Phenomena on the low side of the null. (b) Phenomena increasing to values of dc magnetic field above the null as discussed in the text.

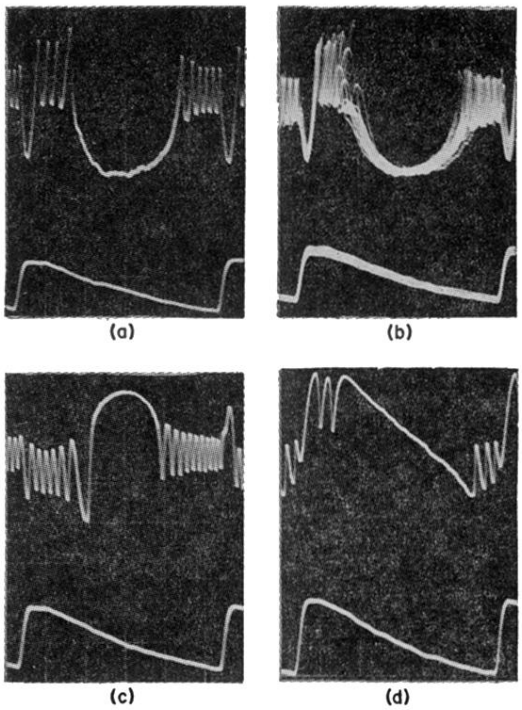

FIG. 5. Sawtooth waveform of magnetic field applied axially on the laser (lower trace of all figures). Frequency 400 cps, 0.36 G peak value. Sweep 0.5 msec/cm. (a) Analyzer along E vector in zero magnetic field. (b) Multiple sweep showing general level of laser stability. (c) Analyzer at 90° to E vector in zero field. (d) Analyzer at 45° to E vector in zero field. Note the circularly polarized beats either side of each response, showing the magnetic field at which coherence is lost.

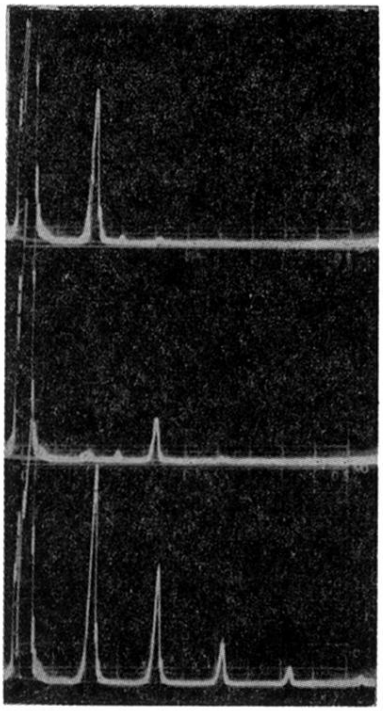

FIG. 6. Modulation due to ac magnetic fields along axis of laser and periodic rotation of polarization. Magnetic field 0.4 G peak, frequency 10 kc/sec. Spectrum analyzer sweep 5 kc/sec/cm, with zero frequency on the left. Upper—analyzer at 45° to E vector in zero field, fundamental component. Middle—analyzer along E vector in zero field; second harmonic produced. Lower—ac magnetic field increased to 1.2 G peak, more harmonic frequency components appear. All components are linearly polarized.

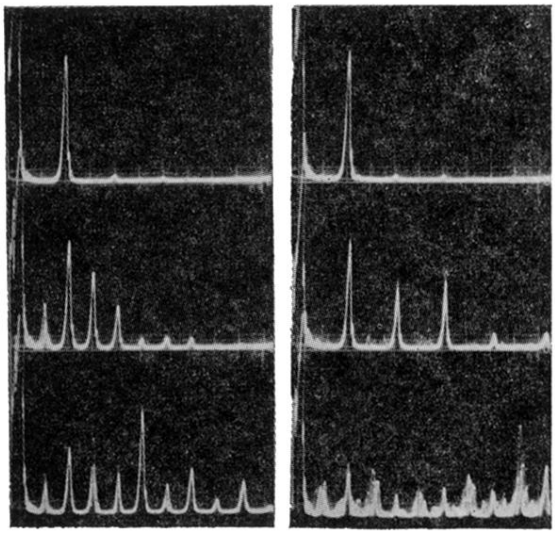

FIG. 9. Subharmonic phenomena at higher amplitudes of the ac magnetic field. (a) Upper—fundamental component at 10 kc/sec, amplitude 0.4 G. Middle and lower traces—components at 5 kc/sec appear—amplitudes of ac magnetic field 0.5 and 1 G, respectively. (b) Similar results—amplitudes of ac field 0.8, 1.4, and 2.5 G from upper to lower traces. Circularly polarized components appear.